Nucleosome Positioning Regulates the Establishment, Stability, and Inheritance of Heterochromatin in *Saccharomyces cerevisiae*

Daniel S. Saxton[a] and Jasper Rine[a,1]

[a]Department of Molecular and Cell Biology, University of California, Berkeley, CA 94720

Edited by Craig S. Pikaard, Indiana University Bloomington, Bloomington, Indiana, and approved September 8, 2020 (received for review March 4, 2020)

Heterochromatic domains are complex structures composed of nucleosome arrays that are bound by silencing factors. This composition raises the possibility that certain configurations of nucleosome arrays facilitate heterochromatic silencing. We tested this possibility in *Saccharomyces cerevisiae* by systematically altering the distance between heterochromatic nucleosome-depleted regions (NDRs), which is predicted to affect local nucleosome positioning by limiting how nucleosomes can be packed between NDRs. Consistent with this prediction, serial deletions that altered the distance between heterochromatic NDRs revealed a striking oscillatory relationship between inter-NDR distance and defects in nucleosome positioning. Furthermore, conditions that caused poor nucleosome positioning also led to defects in both heterochromatin stability and the ability of cells to generate and inherit epigenetic transcriptional states. These findings strongly suggest that nucleosome positioning can contribute to formation and maintenance of functional heterochromatin and point to previously unappreciated roles of NDR positioning within heterochromatic domains.

epigenetics | chromatin | gene silencing

A central challenge to both transcription and transcriptional regulation in eukaryotes is the handling of nucleosomes, the fundamental repeating units of chromatin. Each nucleosome consists of 147 base pairs of DNA wrapped around eight histone subunits, two copies each of histones H2A, H2B, H3, and H4. Nucleosomes can be posttranslationally modified at specific amino acid positions, precisely or poorly positioned, and packaged into higher-order chromatin structures to control gene expression. Nucleosome dynamics are especially relevant in heterochromatin, which is composed of covalently modified nucleosome arrays bound by silencing factors. Despite their importance, it remains unclear exactly how nucleosomes are arranged to create functional heterochromatin.

The interplay between silencing factors and nucleosomes is complex. Formation of heterochromatin generally requires recruitment of silencing factors to specific nucleation sites, and subsequent iterative cycles of histone modification and binding of silencing complexes allow these complexes to spread across nucleosome arrays (1–3). Some silencing factors, including HP1, Sir3, and PRC2, can bridge neighboring nucleosomes, allowing the formation of large chromatin structures (4–6). Additionally, some chromatin remodelers are associated with heterochromatin and required for transcriptional silencing (7, 8). These studies indicate that nucleosomes may be positioned in specific ways to permit heterochromatin formation and maintenance.

The organization of nucleosome arrays is driven by multiple factors. First, different DNA sequences have different intrinsic abilities to bend around a histone octamer, which affects their ability to form nucleosomes (9, 10). Second, nucleosome-depleted regions (NDRs), which are formed by nucleosome-disfavoring DNA sequences or by tightly bound transcription factors, have the ability to position adjacent nucleosomes into phased arrays (11–13). Additionally, two NDRs in close proximity should constrain the number of nucleosomes that can fit between them (14, 15). For example, if two NDRs are spaced approximately two nucleosome lengths apart, then two nucleosomes should fit in that space and be relatively well positioned. Conversely, if two NDRs are two-and-a-half nucleosome lengths apart, then two nucleosomes should still fit in that space but may become more poorly positioned by sampling a greater length of DNA. Indeed, a genome-wide study in *Saccharomyces cerevisiae* found that certain lengths of DNA between NDRs are correlated with, and presumably responsible for, more poorly positioned nucleosomes (16).

If nucleosome positioning affects heterochromatin, then altering inter-NDR distances within heterochromatin could lead to defects in gene silencing. We tested this prediction for two heterochromatic domains in *S. cerevisiae*: *HML* and *HMR*. The *E* and *I* silencers are NDRs that flank each of these domains; each silencer is bound by combinations of the DNA-binding proteins Rap1, Abf1, and ORC (17). These proteins outcompete nucleosomes for binding to silencers (18, 19) and also cooperate to recruit Sir proteins (20, 21). Sir1 is bound only at silencers. In contrast, Sir2/3/4 complexes bind to silencers, spread across the locus, and silence any genes within these domains (1, 2, 22). The bidirectional promoter in *HML* also contains an NDR that is bound by Rap1, and this site likely contributes both to heterochromatic silencing and to transcription when *HML* is unsilenced

Significance

Cells control which genes are actively providing instructions to the cell, and which genes are silenced. This regulation requires DNA to be wrapped around molecular scaffolds to form repeating units called nucleosomes. The organization of nucleosomes varies across the genome, with regular placement being a feature of regions adjacent to nucleosome-depleted regions (NDRs) and irregular positions more common elsewhere. To test whether regular positioning of nucleosomes is especially important in gene silencing, we altered the distance between NDRs within heterochromatin. These changes to NDR positioning revealed an oscillatory correlation between inter-NDR distance and poor nucleosome positioning. These defects in nucleosome positioning correlated with defects in silencing efficiency, indicating that regular placement of nucleosomes helps cells achieve gene silencing.

Author contributions: D.S.S. and J.R. designed research; D.S.S. performed research; D.S.S. analyzed data; and D.S.S. and J.R. wrote the paper.

The authors declare no competing interest.

This article is a PNAS Direct Submission.

[1]To whom correspondence may be addressed. Email: jrine@berkeley.edu.

This article contains supporting information online at https://www.pnas.org/lookup/suppl/doi:10.1073/pnas.2004111117/-/DCSupplemental.

First published October 19, 2020.

(23, 24). Here, we tested whether the precise distance between these NDRs affected nucleosome positioning and, if so, whether effects on positioning affected heterochromatin stability.

Results

Inter-NDR Distance Affected Silencing Stability. In wild-type cells, *HML* and *HMR* are constitutively silenced. Rare, transient loss-of-silencing events can be detected using the Cre-Reported Altered States of Heterochromatin (CRASH) assay (Fig. 1*A*) (25). In this assay, the coding sequence of the *α2* gene in *HML* is replaced with the coding sequence of *cre*, and a cassette consisting of two fluorescent reporter genes with appropriately placed *lox* sites (hereafter referred to as the *lox* cassette) is located elsewhere in the genome. Transient loss of silencing causes *cre* expression, which leads to recombination of the *lox* cassette and an irreversible switch from expressing only red fluorescent protein (RFP) to expressing only green fluorescent protein (GFP). In a colony, the descendants of cells that lost silencing continue expressing GFP and form radial GFP+ sectors during colony growth. Therefore, the apex of each sector represents a single cell that lost silencing, and the number of GFP+ sectors in a colony represents the frequency of loss-of-silencing events.

Consistent with previous studies that utilized micrococcal nuclease (MNase) and histone H3 chromatin immunoprecipitation

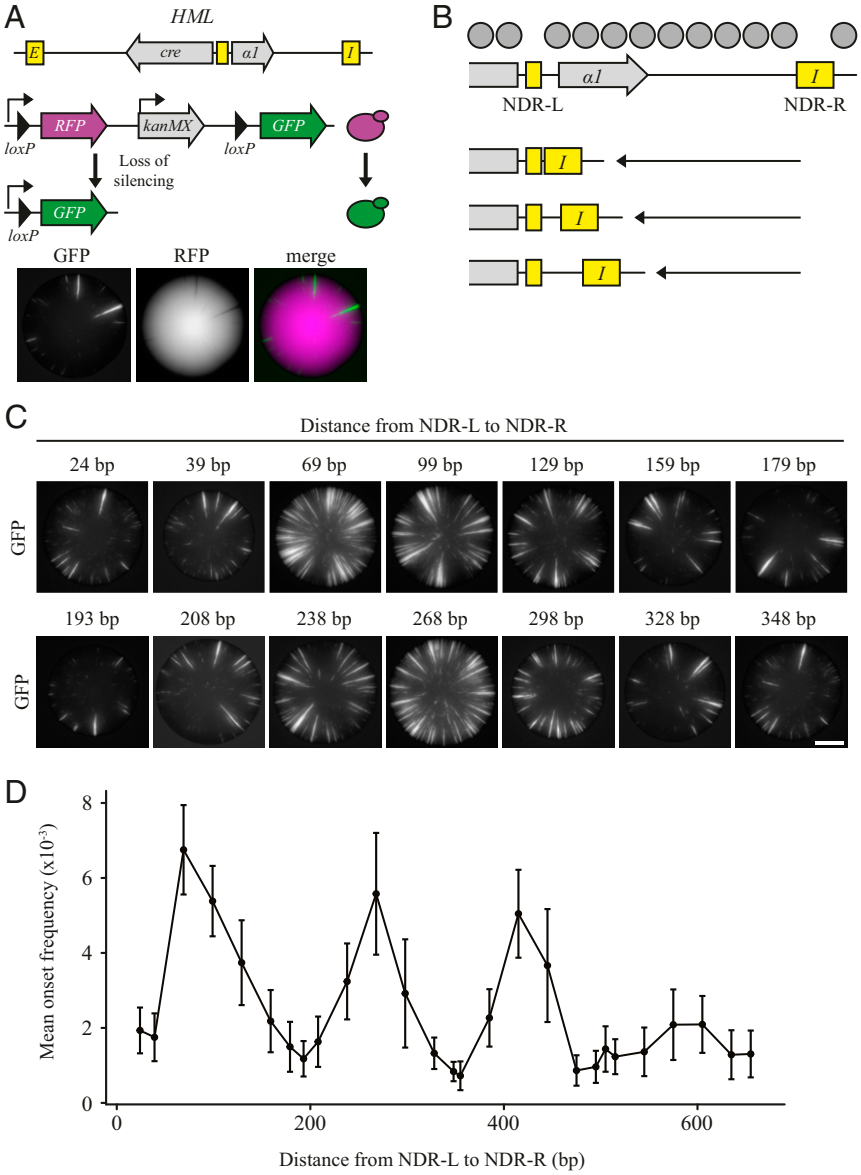

Fig. 1. Inter-NDR distance affected silencing stability. (*A*) Schematic of the CRASH assay (25). In this assay, *cre* replaces the *α2* coding sequence in *HML*. Nucleosome-depleted regions, including the *E* silencer, *I* silencer, and bidirectional promoter, are indicated as yellow boxes. Transient expression of Cre recombines a *lox* cassette elsewhere in the genome, which causes cells to irreversibly switch from expressing RFP to expressing GFP. Therefore, during colony growth, cells that lose silencing lead to formation of GFP+ sectors on an otherwise RFP+ background. (*B*) Schematic of serial deletions used to alter inter-NDR distance. The bidirectional promoter contains a Rap1-binding site and is termed NDR-L. The *HML-I* silencer, which contains binding sites for Abf1, Rap1, and ORC, is termed NDR-R. Nine well-positioned nucleosomes reside between these NDRs (*SI Appendix*, Fig. S1) (gray circles). A series of deletions was made to move NDR-R to various distances from NDR-L (JRY11330-11342, JRY11259, JRY11281, JRY11296, JRY11297, JRY11280, JRY11317-11327). (*C*) Representative CRASH colonies from strains with different inter-NDR distances. The distance between NDR-L and NDR-R is indicated for each strain. (*D*) Sectoring rates were quantified with MORPHE software (26). Data are means ± SD (n = 10 colonies per genotype) (scale bar, 2 mm).

(ChIP), MNase sequencing (MNase-Seq) of *HMLα::cre* revealed the existence of NDRs at the *HML-E* and *HML-I* silencers, as well as at the bidirectional promoter (*SI Appendix*, Fig. S1) (18). Nucleosomes between these NDRs appeared well positioned. To alter inter-NDR distance in *HML*, we generated a series of 28 deletions between the Rap1-binding site in the bidirectional promoter, which we term NDR-L, and the Abf1-binding site in the *HML-I* silencer, which we term NDR-R (Fig. 1*B* and *SI Appendix*, Fig. S1). The largest of these deletions left 24 base pairs between NDR-L and NDR-R, and smaller deletions increased this distance incrementally. The only known DNA elements that were fully or partially deleted in these strains were the *α1* transcription initiation site and the *α1* coding sequence, which are not thought to be involved in expression of *α2* (23).

Strikingly, the frequency of loss-of-silencing events appeared to rise and fall with increasing inter-NDR distances (Fig. 1*C* and *SI Appendix*, Fig. S2). Additionally, these oscillatory effects diminished with increasing inter-NDR distances. We quantified loss-of-silencing rates by using MORphological PHenotype Extraction (MORPHE) software, which calculates the frequency of sectors and their onset points (Fig. 1*D*) (26). Additionally, we quantified loss-of-silencing events by measuring fluorescence of single cells. Cells that have recently lost silencing, and thereby recently recombined the *lox* cassette, contain both RFP and GFP due to a lag time in RFP degradation. By using flow cytometry to measure the frequency of these cells, we also found an oscillatory correlation between inter-NDR distance and silencing-loss rate (*SI Appendix*, Fig. S3). Because these two quantification methods showed similar trends, individual experiments in the rest of this study used one or the other.

Based on the average nucleosome repeat length of 165 base pairs in *S. cerevisiae* (27), we defined one nucleosome "unit" as 165 base pairs. If the distance between NDR-L and NDR-R could be evenly divided into nucleosome units, silencing was more stable than if that distance could not be evenly divided into nucleosome units. For example, an inter-NDR distance of 179 base pairs corresponds to 1.1 nucleosome units, nearly an exact nucleosome unit of 1, and this inter-NDR distance yielded more stable silencing than an inter-NDR distance of 236 base pairs, which corresponds to 1.6 nucleosome units. We estimated the periodicity of changes in silencing-loss rates by calculating the distances between individual peaks, or individual troughs, of silencing-loss rates. These distances averaged to 159 base pairs, similar to the 165 base pairs in a nucleosome unit. This result strongly suggested that the periodicity of silencing-loss rates was correlated with whether or not different inter-NDR distances could be evenly divided into nucleosome units.

In principle, the periodicity of silencing-loss rates was compatible with at least two different mechanisms: one possibility was that inter-NDR distances that were not evenly divisible by nucleosome units resulted in loss of heterochromatin stability. Alternatively, variation in the lengths of the deletions might impact transcription from the bidirectional promoter, which could affect transcription of *cre* in both silenced and unsilenced cells. To test these possibilities, we blocked silencing in a subset of strains with different inter-NDR distances by exposing them to nicotinamide (NAM), a chemical inhibitor of Sir2, and quantified *cre* expression with RT-qPCR. Interestingly, strains which showed large differences in silencing-loss rates with the CRASH assay did not exhibit significant differences in *cre* expression when *HML* was unsilenced (*SI Appendix*, Fig. S4). These results suggested that different lengths between NDR-L and NDR-R affected heterochromatin stability rather than transcription from the bidirectional promoter.

In this framework, silencing was more stable when the distance between NDR-L and NDR-R was evenly divisible by nucleosome units, and less stable when this distance was not evenly divisible by nucleosome units (Fig. 1*D*). These findings raised the possibility that altered nucleosome packing between these NDRs could lead to defects in silencing stability.

Inter-NDR Distance Affected Nucleosome Positioning. To test the expectation that the distance between NDR-L and NDR-R influences silencing stability through effects on nucleosome positioning, we performed MNase-Seq on strains with different distances between these NDRs (Fig. 2). These data represent smoothed midpoints of protected fragments that were between 140 base pairs and 180 base pairs in length. We inferred that these protected fragments reflected nucleosomes, as they correspond to protected fragments in H3 ChIP-Seq experiments. All strains exhibited nucleosome depletion at NDR-L and NDR-R. Additionally, nucleosomes to the left of NDR-L, and to the right of the NDR-R, appeared regularly positioned in most strains. In contrast, nucleosomes between these NDRs exhibited striking differences in positioning and occupancy at various inter-NDR distances.

There were no strongly protected sequences between NDR-L and NDR-R when the distance between these NDRs was at or below 99 base pairs. When this distance was expanded past 99 base pairs, the appearance of a protected sequence became evident. Additionally, the appearance of nucleosomes in this inter-NDR region correlated with a stabilization of silencing until the inter-NDR distance exceeded 193 base pairs. Notably, the protected sequence to the right of NDR-L formed a smaller peak than the same nucleosome seen in *SI Appendix*, Fig. S1, likely reflecting variation in the extent of MNase digestion between different experiments. As the inter-NDR distance expanded beyond 193 base pairs, nucleosome-sized protected fragments were present in the inter-NDR region but appeared to be irregularly positioned in some strains. Generally, inter-NDR distances that were not evenly divisible by nucleosome units exhibited irregularly positioned nucleosomes and stronger silencing defects. These data suggested that inter-NDR distances that were evenly divisible by nucleosome units facilitated silencing stability by allowing proper nucleosome positioning.

NDR-R Was Required for Oscillatory Silencing Effects. The deletions made between NDR-L and NDR-R affected both the DNA sequence content in this region and the relative distances between these NDRs. Either or both of these variables could theoretically contribute to nucleosome positioning and therefore be responsible for the oscillatory effects on silencing stability (Fig. 1). To test the contribution of NDRs to the observed silencing effects, we deleted NDR-R in 14 strains with different distances between NDR-L and NDR-R. Deletion of NDR-L was not feasible due to its role in transcription (23). Deletion of NDR-R led to high overall sectoring rates and eliminated the oscillatory silencing effects (Fig. 3*A* and *SI Appendix*, Fig. S5). Thus, the oscillation in silencing stability reflected the distance between NDR-L and NDR-R rather than some functional properties of the sequences between these NDRs.

Given that NDR-R is a silencer, it was possible that removal of a silencer per se could mask the oscillatory silencing effects independently of its ability to act as an NDR. To test this possibility, we also deleted the *HML-E* silencer in strains with different distances between NDR-L and NDR-R. Oscillatory silencing effects were still observed among strains that lacked the *HML-E* silencer (Fig. 3*B* and *SI Appendix*, Fig. S5). These data further supported the view that the oscillatory silencing effects resulted from changes in distance between NDR-L and NDR-R.

Replacement of NDR-R with Heterologous NDRs. Though the correlation between silencing stability and proper nucleosome positioning suggested a causal relationship between these two variables, it was possible that the observed silencing effects resulted from a separate aspect of NDR repositioning. Previous

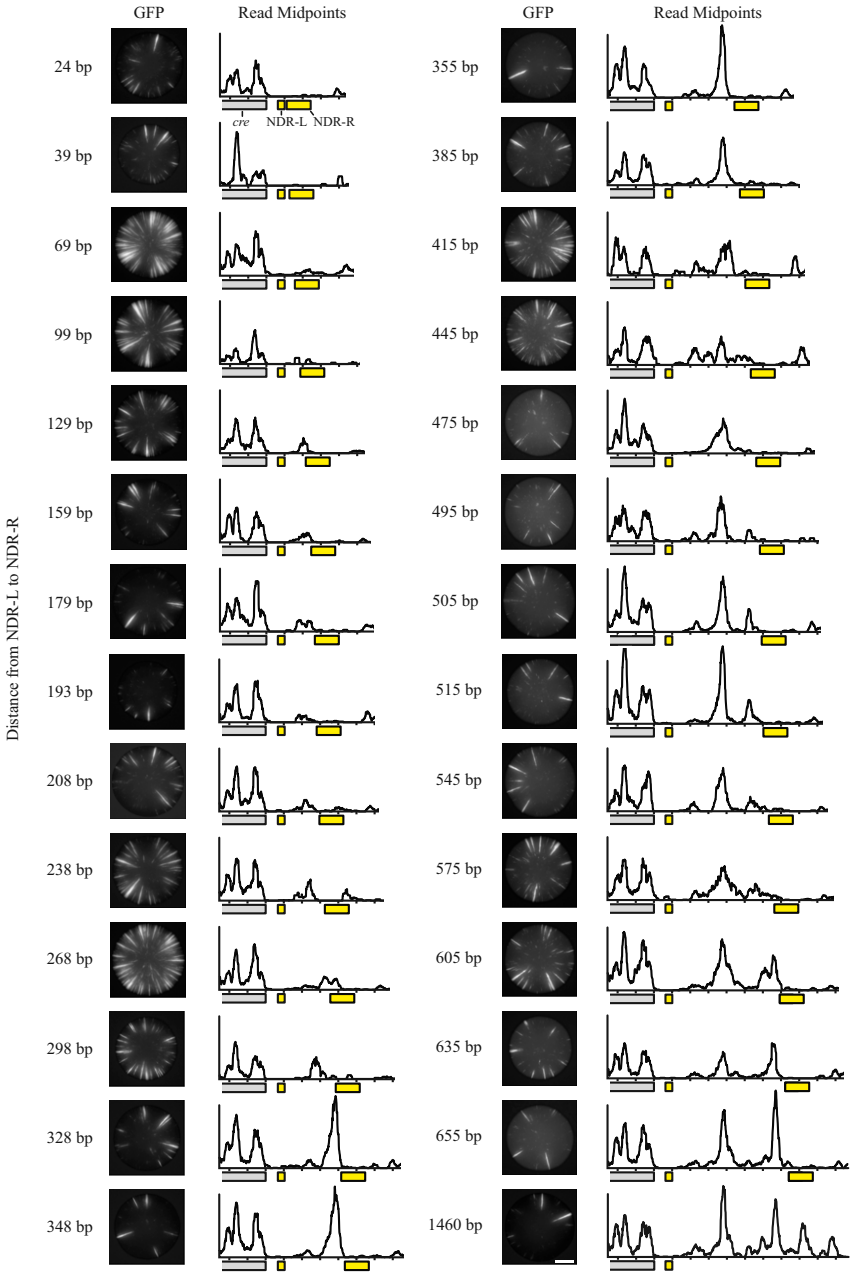

Fig. 2. Inter-NDR distance affected nucleosome positioning. MNase-Seq was used to identify nucleosome positions in strains with different inter-NDR distances (JRY11259, JRY11280, JRY11281, JRY11296, JRY11297, JRY11317-11327, JRY11330-11342). Midpoints of MNase-protected fragments ranging from 140 base pairs to 180 base pairs in length were plotted and smoothed. The relative positions of *cre* (gray box), NDR-L (leftmost yellow box), and NDR-R (rightmost yellow box) are indicated, with tick marks representing 100 base pair intervals. The distance in base pairs between NDR-L and NDR-R is provided for each strain. Representative CRASH colonies from Fig. 1*C* and *SI Appendix*, Fig. S2 are provided for comparison. The strain with 1,460 base pairs between NDR-L and NDR-R contained *HML* lacking any inter-NDR deletions (JRY11259) (scale bar, 2 mm).

studies suggest that silencers at *HM* loci can interact with each other and the bidirectional promoter to form loops, and it is possible that such loops facilitate silencing (28, 29). In this case, different distances between NDR-L and NDR-R may be more amenable or refractory to loop formation between these two sites, which could in turn impact silencing stability. To test this possibility, we replaced NDR-R with either of two heterologous NDRs that have no known roles in silencing (Fig. 4*A*). One of these NDRs consisted of a trio of binding sites for the nucleosome-depleting factor Reb1 (30); these sites were able to efficiently deplete nucleosomes as judged by MNase-qPCR (*SI Appendix*, Fig. S6). The other heterologous NDR consisted of a 100 base pair poly-A sequence, which we utilized based on previous observations that poly-A sequences efficiently deplete nucleosomes in vivo (9, 15). We note that our large poly-A sequence was refractory to analysis of nucleosome occupancy by MNase-qPCR and MNase-Seq.

As with the native NDR-R, different inter-NDR distances between NDR-L and either heterologous NDR resulted in oscillatory silencing effects (Fig. 4 *B* and *C* and *SI Appendix*, Fig. S7). Therefore, given that oscillatory effects were still observed when *HML-I* was replaced with either of two heterologous

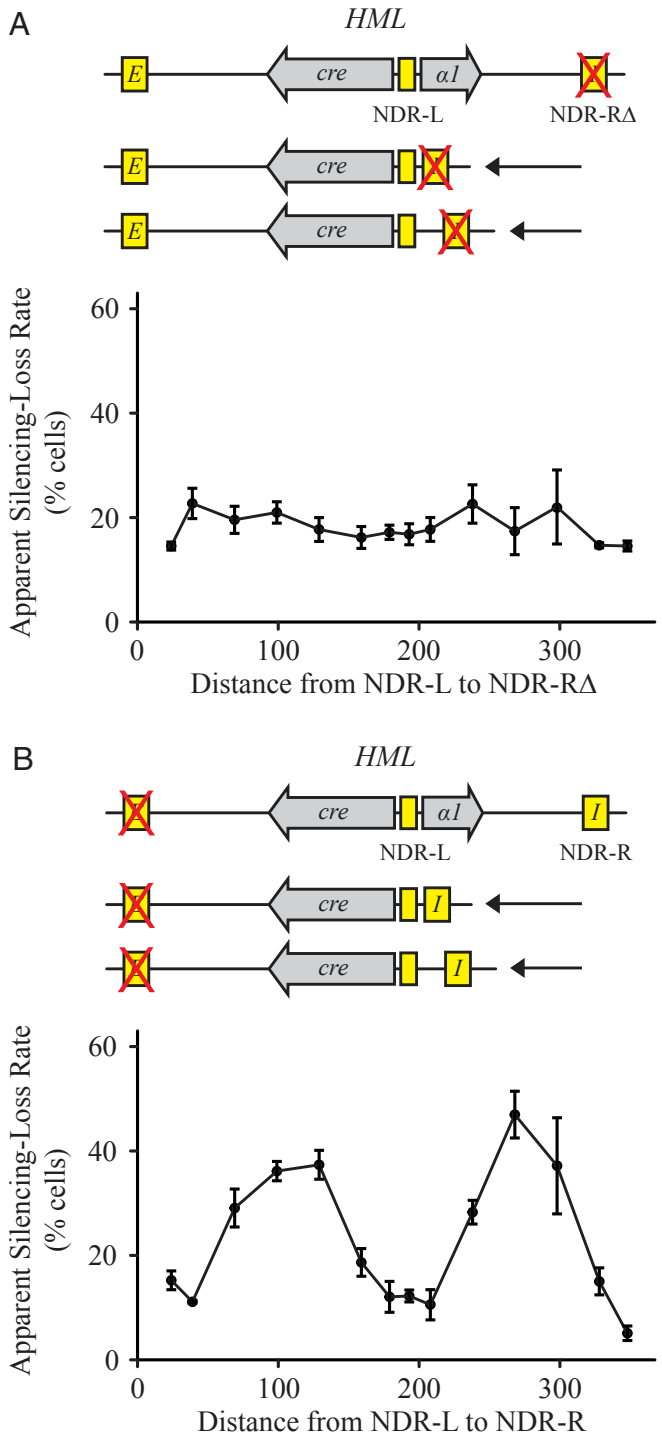

Fig. 3. NDR-R was necessary for oscillatory silencing effects. (*A*) NDR-R was deleted in strains with different inter-NDR distances (JRY11362-11375). Apparent silencing-loss rates were quantified by flow cytometry. Data are means ± SD (n = 3 independent cultures). (*B*) Quantification of apparent silencing-loss rates in strains with different inter-NDR distances and deletion of the *HML-E* silencer, as calculated by flow cytometry (JRY11377-JRY11390). Data are means ± SD (n = 3 independent cultures). Representative CRASH colonies are shown in *SI Appendix*, Fig. S5.

NDRs, we inferred that looping activities involving *HML-I* were not the cause of oscillatory silencing effects. Importantly, both of these heterologous NDRs have transcriptional activation activities (9, 31), and it was possible that a loop with transcriptional activation activity could form between heterologous NDRs and the bidirectional promoter. If this heterologous loop existed and accounted for oscillatory silencing effects, it would also be likely to exhibit oscillatory transcriptional activation effects in unsilenced cells. However, transcription levels of *cre*

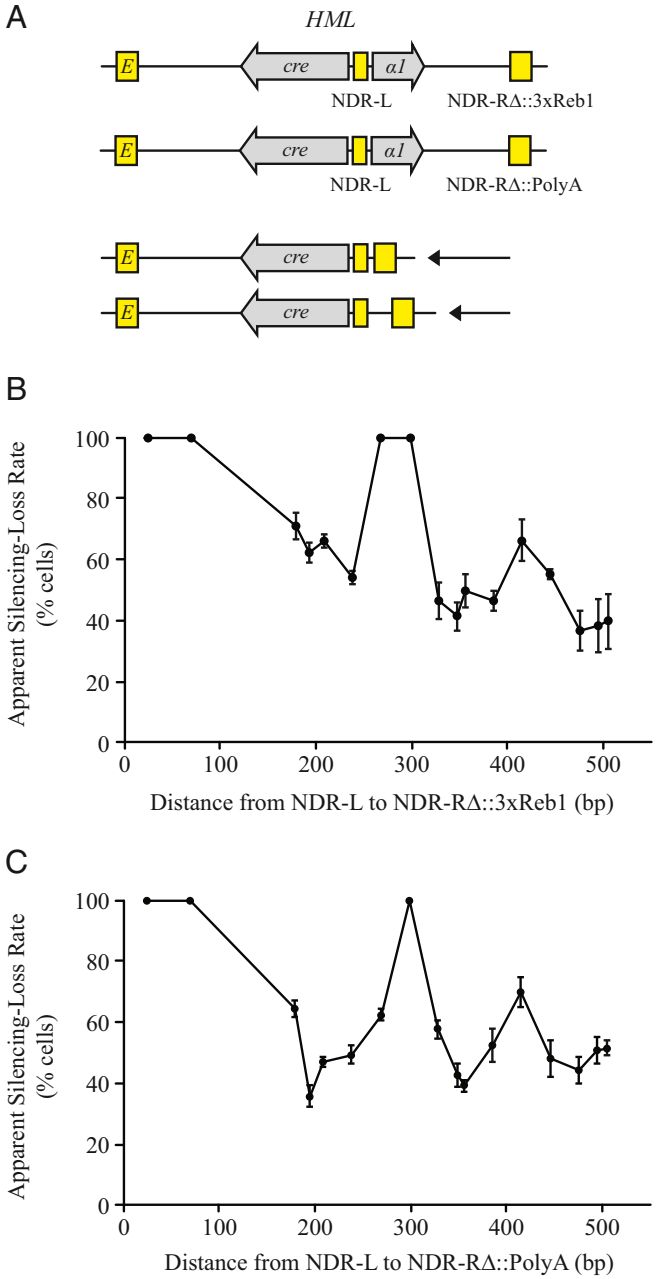

Fig. 4. Oscillatory silencing effects were observed with heterologous NDRs. (*A*) NDR-R was replaced with either a trio of Reb1-binding sites (JRY12961) or a 100 base pair poly-A sequence (JRY12960), and serial deletions were used to change inter-NDR distance (JRY12969-13002). (*B*) Apparent silencing-loss rates for different inter-NDR distances between NDR-L and NDR-RΔ::3xReb1 (JRY12969-12985), as calculated by flow cytometry. (*C*) Apparent silencing-loss rates for different inter-NDR distances between NDR-L and NDR-RΔ::PolyA (JRY12986-13002), as calculated by flow cytometry. Data are means ± SD (n = 6 independent cultures). Silencing-loss rates labeled as 100% reflect strains in which RFP+ cells were not recoverable during strain generation, as described in *Materials and Methods*.

did not exhibit oscillatory changes in unsilenced cells with different distances between NDR-L and the trio of Reb1-binding sites (*SI Appendix*, Fig. S6). Therefore, we inferred that any potential looping functions of NDR-R or heterologous NDRs were not responsible for the oscillatory silencing effects. This finding was consistent with the idea that oscillatory silencing effects were caused by changes in nucleosome positioning.

Contributions of Inter-NDR DNA Content. In addition to the inter-NDR distance, the DNA sequence between NDR-L and NDR-R might also contribute to the observed oscillatory silencing pattern. For example, it was possible that nucleosome positioning affected binding of a sequence-specific DNA-binding protein to its binding site(s) within the inter-NDR region. If this factor affected silencing, then the differential binding of this factor in strains with different inter-NDR distances could conceivably contribute to the oscillatory silencing patterns. The only known motif within the inter-NDR region is the transcription initiation site for the *α1* gene, which resides ~50 base pairs to the right of NDR-L. Notably, when the inter-NDR distance was 39 base pairs or less, then the initiation site was absent and silencing was stable (Fig. 1*C*). However, when the inter-NDR distance was expanded to 69 base pairs, the initiation site was revealed and silencing was less stable. Therefore, it was possible that the initiation site contributed to the oscillatory silencing effects observed in strains with inter-NDR distances of 69 base pairs or greater.

To test if the initiation site contributed to the oscillatory silencing effects, we deleted the DNA corresponding to the nucleosome that contained the initiation site, and subsequently made serial deletions that changed the distance between NDR-L and NDR-R. The resulting strains exhibited oscillatory silencing effects with different inter-NDR distances (*SI Appendix*, Fig. S8). Thus, the transcription initiation site for the *α1* gene was not necessary for the oscillatory silencing effects.

Given that different DNA sequences have different propensities to form nucleosomes (10), it was possible that the oscillatory silencing effects were influenced by the inter-NDR DNA sequence. To test this possibility, we made serial deletions between NDR-L and NDR-R in which the right side of the deletion, which is adjacent to NDR-R, was varied rather than the left side. This effectively created inter-NDR distances similar to those in Figs. 1 and 2, but changed the DNA sequence between the NDRs. The oscillatory silencing effects were still observed in these strains (*SI Appendix*, Fig. S9). These data suggested that the distance between NDRs, rather than the specific DNA sequence between them, was the central driver of observed silencing effects.

Inter-NDR Distance Affected Silencing Stability at *HMRα*. Since all perturbations mentioned thus far were made at *HMLα::cre*, we were curious if nucleosome positioning effects on silencing were specific to *HMLα::cre* or a general feature of heterochromatin. To test this, we employed a variant of the CRASH assay that utilizes a separate heterochromatic domain, *HMRα::cre* (25). Notably, this domain contains the endogenous *HMR* silencers and a fragment from *HMLα::cre* that contains *cre*, the *HML* bidirectional promoter, and the *α1* gene (*SI Appendix*, Fig. S10). A previous study established that the *HML* bidirectional promoter and both *HMR* silencers in *HMRα::cre* are nucleosome depleted, and revealed five well-positioned nucleosomes between the *HML* bidirectional promoter and the *HMR-I* silencer (32). To alter inter-NDR distance, as above, we made a series of 14 deletions between the Rap1-binding site in the *HML* bidirectional promoter, which is termed NDR-L, and the Abf1-binding site in the *HMR-I* silencer, which is termed NDR-R. These mutants exhibited oscillatory silencing effects similar to those seen at *HMLα::cre*, albeit dampened in strains with inter-NDR distances greater than 200 base pairs (*SI Appendix*, Fig. S10). Thus, nucleosome positioning contributed to silencing stability in a second heterochromatic domain.

Inter-NDR Distance Influenced Epigenetic Inheritance. It is possible that nucleosome positioning affects both transient loss-of-silencing events, as measured by the CRASH assay, and transmission of epigenetic chromatin states. In the absence of Sir1, genetically identical cells can be either transcriptionally silenced or expressed at individual heterochromatic mating-type loci. These transcriptional states are heritable and switching events between states can be monitored with the FLuorescent Assessment of Metastable Expression (FLAME) assay (32). This assay utilizes *HMLα::RFP* or *HMRα::GFP* in a *sir1Δ* mutant, and fluorescence profiles of cells can be monitored with flow cytometry and microscopy. Since *HMRα::GFP* is silenced more frequently than *HMLα::RFP*, *HMRα::GFP* provides a better dynamic range to measure potential silencing defects.

To test the effects of nucleosome positioning on epigenetic states, we altered the distance between NDR-L and NDR-R in *HMRα::GFP* and calculated the frequency of different epigenetic states by using flow cytometry (Fig. 5 *A* and *B*). Strikingly, the frequency of silenced cells exhibited an oscillatory pattern; strains with inter-NDR distances that were evenly divisible by nucleosome units had more silenced cells, and strains with distances that were not evenly divisible by nucleosome units had more expressed cells (Fig. 5 *C* and *D*). These results suggested that switching rates between states varied in strains with different inter-NDR distances. Indeed, by using time-lapse microscopy to monitor switching events in dividing cells, we found that the rate of silencing loss was higher for inter-NDR distances that were not evenly divisible by nucleosome units (Fig. 5*E*). Interestingly, these same strains also exhibited a lower rate of silencing establishment (Fig. 5*F*). These data suggested that proper nucleosome positioning facilitates both establishment and inheritance of the silenced epigenetic state at *HMR*.

Discussion

Heterochromatin is a complex structure that usually requires cooperation between modified nucleosome arrays and silencing proteins. Though this cooperative nature suggests that specific configurations of nucleosome arrays may be required for effective silencing, strong evidence for this idea has been lacking. Here, we tested whether nucleosome positioning within heterochromatin affects silencing stability by altering the distance between heterochromatic NDRs. We found that well-localized nucleosomes contribute to silencing stability in two heterochromatic domains and facilitate the establishment, stability, and heritability of epigenetic silenced states.

Effects of Inter-NDR Distance on Nucleosome Positioning. The barrier model of nucleosome positioning posits that NDRs act as barriers to nucleosome movement and effectively constrain the positions of adjacent nucleosomes (14). This model has been supported by evidence that nucleosomes are usually well positioned near NDRs and more poorly positioned at locations distant from NDRs (15). Indeed, in contrast to yeast, the much larger human genome has more poorly positioned nucleosomes due to the large amount of space between NDRs at promoters, enhancers, and other regulatory sites (33).

A corollary of the barrier model is that two NDRs in close proximity should constrain the number of nucleosomes that can fit between them. Consistent with this idea, a genome-wide study found that inter-NDR distances that are evenly divisible by nucleosome units have relatively well-positioned nucleosomes in that space, whereas those that are not evenly divisible by nucleosome units correspond to more poorly positioned nucleosomes (16). Our results built on these findings by showing that changes in

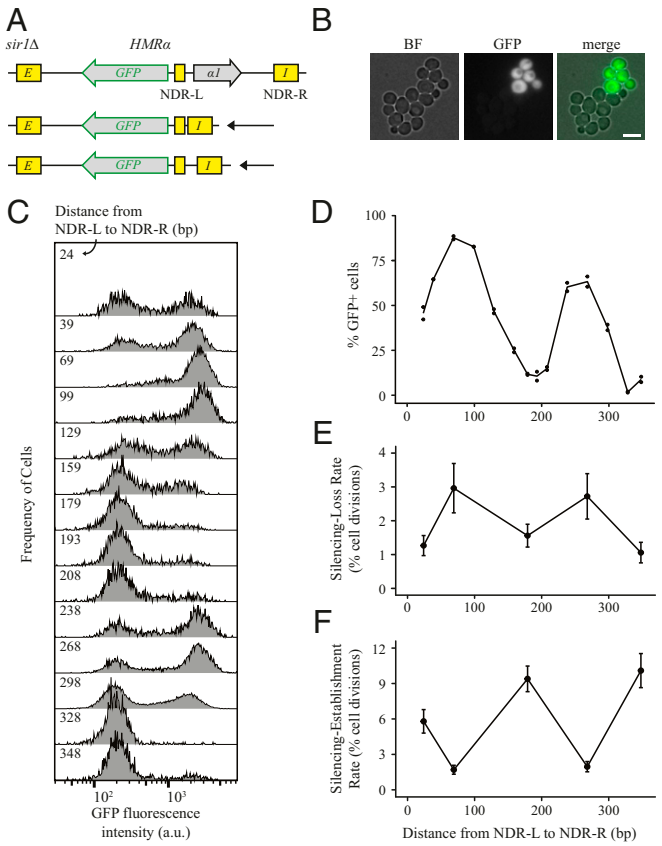

Fig. 5. Inter-NDR distance influenced transmission of epigenetic states in *sir1Δ*. (*A*) Schematic of the FLAME assay (32). In this assay, *GFP* replaces the *α2* gene in *HMRα* in a *sir1Δ* genetic background. NDRs are depicted as yellow boxes, including *HMR-E*, the *HML* bidirectional promoter (NDR-L), and the *HMR-I* silencer (NDR-R). (*B*) Epigenetic states of *HMRα* observed with live-cell microscopy (JRY11478). (*C*) Frequency of silenced and expressed cells in strains with different inter-NDR distances (JRY11543, JRY12306-12318). Serial deletions identical to those made in *SI Appendix*, Fig. S10 were used to alter the distance between NDR-L and NDR-R. Cells were grown at log-phase for 48 h to reach equilibrium, and subsequently analyzed by flow cytometry. (*D*) Quantification of the frequency of expressed cells observed by flow cytometry in *C*. Data points represent independent cultures ($n = 2$ per strain) and the line represents the mean for each strain. (*E*) Quantification of silencing-loss rates observed with time-lapse microscopy ($n > 500$ cell divisions per genotype) for a subset of strains (JRY11543, JRY12307, JRY12312, JRY12315, JRY12318). (*F*) Quantification of silencing-establishment rates observed with time-lapse microscopy ($n > 400$ cell divisions per genotype) for the same subset of strains (JRY11543, JRY12307, JRY12312, JRY12315, JRY12318). Error bars represent 95% confidence intervals (scale bar, 5 μm).

inter-NDR distance at a specific locus of interest influenced nucleosome array patterns, with the most well-positioned nucleosomes corresponding to inter-NDR distances that are evenly divisible by nucleosome units.

Contributions of Nucleosome Positioning to Heterochromatin Stability. A simple model for the observed oscillatory silencing effects is that poor nucleosome positioning within heterochromatin leads to relatively large gaps between nucleosomes, which in turn causes silencing defects. In this view, inter-NDR distances that are not evenly divisible by nucleosome units would contain the permissible number of nucleosomes, but the inability to make all of the DNA nucleosomal would lead to gaps of unoccupied DNA that destabilize silencing. In support of this idea, the ability of the *HML-I* silencer to silence a nearby reporter gene is blocked by the introduction of a nucleosome-disfavoring DNA sequence between these two sites (34). Similarly, the incorporation of heterologous nucleosomal DNA sequences with long linker regions into *HML* is less permissible to silencing than incorporation of the same DNA sequences with short linker regions (35).

Poorly positioned nucleosomes and nucleosome-free DNA could destabilize heterochromatin for multiple reasons. Previous work found that disruption of chromatin remodelers can lead to genome-wide defects in nucleosome positioning and increased levels of cryptic transcription (36, 37). Considering that the *HMLα1* initiation site is normally nucleosomal and not leading to active transcription, it was possible that irregular nucleosome positioning over this site led to aberrant transcription and subsequent destabilization of local heterochromatin. However, two independent experiments established that the *HMLα1* initiation site was not necessary for the observed oscillatory silencing effects (*SI Appendix*, Figs. S8 and S9).

An alternative possibility is that the spreading of silencing factors is limited by gaps of nucleosome-free DNA. Consistent with this idea, nucleosome-disfavoring DNA sequences are able to partially block the spread of Sir proteins from *HML-I* silencer (34). In theory, increased distances between nucleosomes could hinder binding of Sir3, which preferentially binds to dinucleosomes in vitro (4). It is also possible that gaps of nucleosome-free DNA can hinder the iterative rounds of H4K16 deacetylation by Sir2 and histone binding by Sir3 that are thought to promote spreading of the Sir complex (1). Further studies will be needed to identify why altered nucleosome positioning and associated gaps between nucleosomes lead to unstable silencing.

It is important to note that the oscillatory silencing effects diminished with longer inter-NDR distances. This observation may suggest that perturbations to nucleosome positioning, and any resulting effects on silencing, can be mitigated by having larger inter-NDR distances. For example, larger inter-NDR distances facilitate the formation of larger nucleosome arrays, which could mitigate the effects of a fixed amount of non-nucleosomal DNA (such as that generated by an inter-NDR distance that is not evenly divisible by nucleosome units) by distributing it over more spaces between individual nucleosomes. This idea is interesting given that heterochromatic domains are often much larger than the repressed genes within them (38–40), and that NDRs such as silencer elements and the bidirectional promoter in *HML* are located relatively far away from each other. Our findings may suggest that this naturally occurring chromatin architecture acts to buffer silencing against processes that transiently disrupt nucleosome positioning, such as DNA replication and DNA repair (41, 42). Additional studies that test how heterochromatic nucleosome arrays can absorb changes in nucleosome positioning may point to advantages of naturally occurring heterochromatin architectures.

Effects of Nucleosome Positioning on Epigenetic States. A central question in chromatin biology is how genetically identical cells can exhibit different, heritable transcriptional states. This epigenetic phenomenon is frequently observed in heterochromatin, raising the question of how silenced transcriptional states can be generated and inherited. One possibility is that some nucleosome array configurations can favor chromatin structures required for different transcriptional states, such as the silenced and expressed states of *HML* and *HMR* in *sir1Δ*. In support of this idea, removal of the linker histone homolog Hho1 causes *HML* to be silenced more frequently in *sir1Δ* strains (43). Similarly, defects in the chromatin remodeling complex Isw2/yCHRAC cause more cells to be silenced at a reporter gene integrated in a synthetic yeast telomere (44).

We built on these findings by testing the effects of inter-NDR distance on epigenetic states of *HMR* in *sir1Δ*. Interestingly,

inter-NDR distances that weren't evenly divisible by nucleosome units led to both higher silencing-loss rates and lower silencing-establishment rates. This result is partially consistent with the earlier discovery that Isw2/yCHRAC contributes only to the silencing-establishment rate at a synthetic yeast telomere (44). Together, these findings argue that poorly positioned nucleosome arrays provide a poor substrate to establish silencing and can lead to defects in inheritance of silencing in some contexts. Additional studies will improve our understanding of why certain nucleosome array patterns are more permissible to specific epigenetic transcriptional states.

Potential Effects of Inter-NDR Distance in Disease Contexts and Synthetic Biology. These observations that inter-NDR distance affects local nucleosome arrays have additional functional implications. Genome wide, inter-NDR distances that are not evenly divisible by nucleosome units correspond to higher histone turnover, higher PolII density, and higher transcriptional plasticity (16). These effects may be relevant to diseases that involve trinucleotide repeat expansions, many of which occur in noncoding regions and have unclear molecular consequences (45). As such, repeat expansions that influence inter-NDR distance, and thereby alter nucleosome positioning, may contribute to some pathologies. Additionally, future experiments that utilize synthetic biology to manipulate chromatin architecture may benefit from the knowledge that different inter-NDR distances can affect transcriptional regulation. This may be especially useful for fine-tuning transcriptional outputs in sensitive regulatory circuits. Further research will be needed to address the relevance of NDR positioning in disease contexts such as trinucleotide repeat expansions and in the field of synthetic biology.

Materials and Methods

Yeast Strains. Strains and oligonucleotides used in this study are listed *SI Appendix*, Table S1. All strains were derived from the W303 background. Strains used in the CRASH and FLAME assays were generated as described previously (25, 32).

All deletions were made with CRISPR/Cas9 technology (46). Each deletion required a single guide RNA (sgRNA) and two oligonucleotides, which are listed in *SI Appendix*, Table S1. The sgRNA was designed to target a site within the region that would be deleted. The two oligonucleotides used for each deletion were partially overlapping and amplified by PCR prior to use. The resulting extended oligonucleotide constituted a repair template that would yield a deletion. Cotransformation of the sgRNA- and Cas9-containing plasmid, as well as the extended oligonucleotide, resulted in transformants with the desired deletion. Deletions were confirmed by junction PCR and sequencing.

To generate strains that replaced the *HML-I* silencer with a trio of Reb1-binding sites or a poly-A sequence, ultramers with the appropriate sequences were amplified and used as repair templates with the appropriate sgRNA- and Cas9-containing plasmid. The ultramer for the trio of Reb1 sites was 5′-GTTTGACTTCTATGTTAACTTACTTCAACATGAAAGCCCGGTTACCCG-GGTTAACATGTAGCCCGGCCCTATTAGTACAGCAGTGCCTTGGTTACCCGGAAT-GACATTCTCATTATTAAATTTTCTCTACAGCCAAACGAGTTACCCGGCGCCGGA-GGTGCTGGAAATGGCAAACGAAAATACTATGAC-3′ and the ultramer for the poly-A sequence was 5′-GTTTGACTTCTATGTTAACTTACTTCAACATGAAAGCCC-GAAAAAAAAAAAAAAAAAAAAAAAAAAAAAAAAAAAAAAAAAAAAAAAA-AAAAAAAAAAAAAAAAAAAAAAAAAAAAAAAAAAAAAAAAAAAAAAAA-AAAAACGCCGGAGGTGCTGGAAATGGCAAACGAAAATACTATGAC-3′. The primers and sgRNA sequences are listed in *SI Appendix*, Table S1. The Reb1 consensus sequence GTTACCCGG was used (47) and the three Reb1 sites were each spaced 40 base pairs apart. Insertions were confirmed by junction PCR and sequencing.

When *HML-IΔ::3xReb1* or *HML-IΔ::PolyA* were generated in strains with different inter-NDR distances, a subset of transformations yielded only colonies that were RFP- GFP+. This result suggested that the resulting genotype had such unstable silencing that recovery of RFP+ cells was impossible or extremely difficult. We tested this by confirming the correct genotype of at least 10 colonies that had the correct repair event and were RFP- and GFP+. Additionally, a significant number of colonies on control plates without a repair template were RFP+, demonstrating that RFP+ cells had indeed been used in the transformation and that an immediate switch to GFP+ had probably occurred in correct transformants.

CRASH Assay. To generate colonies, cells were plated at a density of ∼10 cells/plate [CSM-Trp (Sunrise Science Products), 1% agar] and grown into colonies over 3 to 4 d. Colonies were imaged with a Leica M205 FA fluorescence stereomicroscope (Leica Camera AG) equipped with a DFC3000G charge-coupled device (CCD) camera, a Leica PLANAPO 0.63× objective, ET RFP filter (Leica 10450224), ET GFP filter (Leica 10447408), and Leica Application Suite X (LAS X) imaging software. A minimum of 10 colonies were imaged per genotype.

Quantification of sectoring rates with MORPHE software was performed as previously described (26). As the onset point of each sector in a colony represented a single silencing-loss event, an average onset frequency for all sectors was calculated for each colony. At least 10 colonies were analyzed per genotype.

To quantify apparent silencing-loss rates by flow cytometry, cells were first inoculated in liquid media (CSM -Trp) and grown to saturation overnight. These cultures were subsequently back-diluted in CSM-Trp, grown at log-phase for 4 h, and analyzed with a BD LSRFortessa cell analyzer (BD Biosciences) with a fluorescein isothiocyanate (FITC) filter and R-PhycoErythrin (PE)-TexasRed filter. Subsequent analysis was performed with FlowJo software. Distinct populations of RFP+ GFP- cells (which had not lost silencing), RFP+ GFP+ cells (which had recently lost silencing), and RFP- GFP+ cells (which had lost silencing less recently) were observed. The apparent silencing-loss rate was calculated by dividing the frequency of RFP+ GFP+ cells by the combined frequencies of RFP+ GFP- and RFP+ GFP+ cells. Apparent silencing-loss rates were calculated for three independent cultures per genotype.

FLAME Assay. Two independent cultures for each strain were grown in liquid media (CSM) to saturation overnight. These cultures were then grown at log-phase for 48 h by repeated serial back-dilutions, ultimately allowing each population to reach an equilibrium of silenced and unsilenced cells.

First, samples from each culture were analyzed by flow cytometry. The frequencies of silenced and unsilenced cells were similar between both independent cultures for each strain, therefore representative flow cytometry profiles were shown for only one culture per strain in Fig. 5*C*. Second, samples from a subset of the cultures were used for time-lapse microscopy as previously described (32). Briefly, cells were sonicated and placed between an agar pad (CSM) and a glass coverslip. Time-lapse imaging was subsequently performed using a Z1 inverted fluorescence microscope (Zeiss). Cells were kept at 30 °C and images were taken every 10 min for 10 h. In subsequent analysis, cell divisions and switching events between epigenetic states were manually counted and the counter was blind to the genotype (single-blind study).

Expression Levels by RT-qPCR. Cells were grown to log-phase in liquid media (CSM) and RNA was extracted with a RNeasy Kit (Qiagen) that included treatment with DNaseI (Qiagen). Reverse transcription was performed using the Invitrogen SuperScript III kit (Invitrogen) and oligo (dT) primers. Quantitative PCR was performed with the DyNAmo HS SYBR Green kit (Thermo Fischer Scientific) on an Mx3000P machine (Stratagene) using two primers for *cre*: 5′-CGTACTGACGGTGGGAGAAT-3′ and 5′-CCCGGCAAAACA-GGTAGTTA-3′. Primers for *ACT1* were used for a control: 5′-TGTCCTTGTACT-CTTCCGGT-3′ and 5′-CCGGCCAAATCGATTCTCAA-3′. Samples were analyzed in technical triplicate for three independent RNA preparations per strain.

MNase-Seq and MNase-qPCR. MNase digestion was performed as previously described (32). Briefly, cultures were grown to log-phase in CSM liquid media and spheroplasted. Nuclei were subsequently purified and treated with MNase (Worthington Biochemical Corporation). Mononucleosomes were isolated and nucleosomal DNA was purified. For MNase-Seq, MNase libraries were constructed with a NEBnextUltra II library preparation kit (New England Biolabs) and sequenced on a HiSeq4000 (Illumina) as 100 base pair paired-end reads. Reads were mapped to the *S. cerevisiae* S288C genome (GenBank accession number GCA_000146045.2) using Bowtie2 (48). Mapped reads between 140 base pairs and 180 base pairs in length were used to provide mononucleosome resolution. Midpoints were calculated for each read and stacked in a histogram. Finally, a 25 base pair rolling mean was used to smooth the histogram of nucleosome peaks. All sequences and processed data files have been deposited in the National Center for Biotechnology Information (NCBI) Gene Expression Omnibus archive under accession number GSE144808. For MNase-qPCR, purified nucleosomal DNA was amplified by stacked primer sets that made ∼100

base pair amplicons and were spaced ~30 base pairs, as previously described (49). To control for different amplification efficiencies, each primer pair was also used to amplify genomic DNA (gDNA). Purified nucleosomal DNA and purified gDNA were each amplified in technical triplicate for each primer pair.

Data Availability. Sequencing information data have been deposited into the publicly available NCBI Gene Expression Omnibus (GSE144808). All study data are included in the article and supporting information.

ACKNOWLEDGMENTS. We thank Lu Bai, Tim Formosa, David Stillman, and Dana Carroll for thoughtful discussions that contributed to this work. We also thank the University of California (UC) Berkeley Flow Cytometry Facility for use of flow cytometers. This work used the Vincent J Coates Genomics Sequencing Laboratory at UC Berkeley, supported by NIH S10 OD018174 Instrumentation Grant. Finally, we thank the Rine lab members for discussions and critical analysis of this work, especially Davis Goodnight, Molly Brothers, Eliana Bondra, Marc Fouet, and Delaney Farris. This work was supported by grants from the NIH (GM31105 and GM120374 to J.R.) and by an NSF predoctoral fellowship (DGE1752814 to D.S.S.).

1. L. N. Rusché, A. L. Kirchmaier, J. Rine, Ordered nucleation and spreading of silenced chromatin in Saccharomyces cerevisiae. *Mol. Biol. Cell* **13**, 2207–2222 (2002).
2. G. J. Hoppe *et al*., Steps in assembly of silent chromatin in yeast: Sir3-independent binding of a Sir2/Sir4 complex to silencers and role for Sir2-dependent deacetylation. *Mol. Cell. Biol.* **22**, 4167–4180 (2002).
3. I. M. Hall *et al*., Establishment and maintenance of a heterochromatin domain. *Science* **297**, 2232–2237 (2002).
4. R. Behrouzi *et al*., Heterochromatin assembly by interrupted Sir3 bridges across neighboring nucleosomes. *eLife* **5**, e17556 (2016).
5. S. Machida *et al*., Structural basis of heterochromatin formation by human HP1. *Mol. Cell* **69**, 385–397.e8 (2018).
6. S. Poepsel, V. Kasinath, E. Nogales, Cryo-EM structures of PRC2 simultaneously engaged with two functionally distinct nucleosomes. *Nat. Struct. Mol. Biol.* **25**, 154–162 (2018).
7. Q. Yu, X. Zhang, X. Bi, Roles of chromatin remodeling factors in the formation and maintenance of heterochromatin structure. *J. Biol. Chem.* **286**, 14659–14669 (2011).
8. K. M. Creamer *et al*., The Mi-2 homolog Mit1 actively positions nucleosomes within heterochromatin to suppress transcription. *Mol. Cell. Biol.* **34**, 2046–2061 (2014).
9. V. Iyer, K. Struhl, Poly(dA:dT), a ubiquitous promoter element that stimulates transcription via its intrinsic DNA structure. *EMBO J.* **14**, 2570–2579 (1995).
10. E. Segal *et al*., A genomic code for nucleosome positioning. *Nature* **442**, 772–778 (2006).
11. N. Kaplan *et al*., The DNA-encoded nucleosome organization of a eukaryotic genome. *Nature* **458**, 362–366 (2009).
12. G. Badis *et al*., A library of yeast transcription factor motifs reveals a widespread function for Rsc3 in targeting nucleosome exclusion at promoters. *Mol. Cell* **32**, 878–887 (2008).
13. T. N. Mavrich *et al*., A barrier nucleosome model for statistical positioning of nucleosomes throughout the yeast genome. *Genome Res.* **18**, 1073–1083 (2008).
14. R. D. Kornberg, L. Stryer, Statistical distributions of nucleosomes: Nonrandom locations by a stochastic mechanism. *Nucleic Acids Res.* **16**, 6677–6690 (1988).
15. G.-C. Yuan *et al*., Genome-scale identification of nucleosome positions in S. cerevisiae. *Science* **309**, 626–630 (2005).
16. C. Vaillant *et al*., A novel strategy of transcription regulation by intragenic nucleosome ordering. *Genome Res.* **20**, 59–67 (2010).
17. A. R. Buchman, W. J. Kimmerly, J. Rine, R. D. Kornberg, Two DNA-binding factors recognize specific sequences at silencers, upstream activating sequences, autonomously replicating sequences, and telomeres in *Saccharomyces cerevisiae*. *Mol. Cell. Biol.* **8**, 210–225 (1988).
18. K. Weiss, R. T. Simpson, High-resolution structural analysis of chromatin at specific loci: Saccharomyces cerevisiae silent mating type locus HMLalpha. *Mol. Cell. Biol.* **18**, 5392–5403 (1998).
19. A. Ravindra, K. Weiss, R. T. Simpson, High-resolution structural analysis of chromatin at specific loci: Saccharomyces cerevisiae silent mating-type locus HMRa. *Mol. Cell. Biol.* **19**, 7944–7950 (1999).
20. T. Triolo, R. Sternglanz, Role of interactions between the origin recognition complex and SIR1 in transcriptional silencing. *Nature* **381**, 251–253 (1996).
21. P. Moretti, K. Freeman, L. Coodly, D. Shore, Evidence that a complex of SIR proteins interacts with the silencer and telomere-binding protein RAP1. *Genes Dev.* **8**, 2257–2269 (1994).
22. A. A. Carmen, L. Milne, M. Grunstein, Acetylation of the yeast histone H4 N terminus regulates its binding to heterochromatin protein SIR3. *J. Biol. Chem.* **277**, 4778–4781 (2002).
23. P. G. Siliciano, K. Tatchell, Transcription and regulatory signals at the mating type locus in yeast. *Cell* **37**, 969–978 (1984).
24. T. H. Cheng, M. R. Gartenberg, Yeast heterochromatin is a dynamic structure that requires silencers continuously. *Genes Dev.* **14**, 452–463 (2000).
25. A. E. Dodson, J. Rine, Heritable capture of heterochromatin dynamics in Saccharomyces cerevisiae. *eLife* **4**, e05007 (2015).
26. T.-Y. Liu, A. E. Dodson, J. Terhorst, Y. S. Song, J. Rine, Riches of phenotype computationally extracted from microbial colonies. *Proc. Natl. Acad. Sci. U.S.A.* **113**, E2822–E2831 (2016).
27. J. Ocampo, R. V. Chereji, P. R. Eriksson, D. J. Clark, The ISW1 and CHD1 ATP-dependent chromatin remodelers compete to set nucleosome spacing in vivo. *Nucleic Acids Res.* **44**, 4625–4635 (2016).
28. J. F.-X. Hofmann, T. Laroche, A. H. Brand, S. M. Gasser, RAP-1 factor is necessary for DNA loop formation in vitro at the silent mating type locus HML. *Cell* **57**, 725–737 (1989).
29. L. Valenzuela, N. Dhillon, R. N. Dubey, M. R. Gartenberg, R. T. Kamakaka, Long-range communication between the silencers of HMR. *Mol. Cell. Biol.* **28**, 1924–1935 (2008).
30. M. J. Fedor, N. F. Lue, R. D. Kornberg, Statistical positioning of nucleosomes by specific protein-binding to an upstream activating sequence in yeast. *J. Mol. Biol.* **204**, 109–127 (1988).
31. D. I. Chasman *et al*., A yeast protein that influences the chromatin structure of UASG and functions as a powerful auxiliary gene activator. *Genes Dev.* **4**, 503–514 (1990).
32. D. S. Saxton, J. Rine, Epigenetic memory independent of symmetric histone inheritance. *eLife* **8**, 585 (2019).
33. D. E. Schones *et al*., Dynamic regulation of nucleosome positioning in the human genome. *Cell* **132**, 887–898 (2008).
34. X. Bi, Q. Yu, J. J. Sandmeier, Y. Zou, Formation of boundaries of transcriptionally silent chromatin by nucleosome-excluding structures. *Mol. Cell. Biol.* **24**, 2118–2131 (2004).
35. S. A. Chakraborty, A. A. Kazi, T. M. Khan, S. G. Genetics, Nucleosome-positioning sequence repeats impact chromatin silencing in yeast minichromosomes. *Genet. Soc. America* **198**, 1015–1029 (2014).
36. V. Cheung *et al*., Chromatin- and transcription-related factors repress transcription from within coding regions throughout the Saccharomyces cerevisiae genome. *PLoS Biol.* **6**, e277 (2008).
37. B. P. Hennig, K. Bendrin, Y. Zhou, T. Fischer, Chd1 chromatin remodelers maintain nucleosome organization and repress cryptic transcription. *EMBO Rep.* **13**, 997–1003 (2012).
38. A. Hecht, S. Strahl-Bolsinger, M. Grunstein, Spreading of transcriptional repressor SIR3 from telomeric heterochromatin. *Nature* **383**, 92–96 (1996).
39. K Noma, C. D. Allis, S. I. S. Grewal, Transitions in distinct histone H3 methylation patterns at the heterochromatin domain boundaries. *Science* **293**, 1150–1155 (2001).
40. Y. B. Schwartz *et al*., Genome-wide analysis of Polycomb targets in Drosophila melanogaster. *Nat. Genet.* **38**, 700–705 (2006).
41. M. J. Smerdon, M. W. Lieberman, Nucleosome rearrangement in human chromatin during UV-induced DNA- reapir synthesis. *Proc. Natl. Acad. Sci. U.S.A.* **75**, 4238–4241 (1978).
42. P. Vasseur *et al*., Dynamics of nucleosome positioning maturation following genomic replication. *Cell Rep.* **16**, 2651–2665 (2016).
43. Q. Yu *et al*., Saccharomyces cerevisiae linker histone Hho1p functionally interacts with core histone H4 and negatively regulates the establishment of transcriptionally silent chromatin. *J. Biol. Chem.* **284**, 740–750 (2009).
44. T. Iida, H. Araki, Noncompetitive counteractions of DNA polymerase epsilon and ISW2/yCHRAC for epigenetic inheritance of telomere position effect in Saccharomyces cerevisiae. *Mol. Cell. Biol.* **24**, 217–227 (2004).
45. C. T. McMurray, Mechanisms of trinucleotide repeat instability during human development. *Nat. Rev. Genet.* **11**, 786–799 (2010).
46. M. E. Lee, W. C. DeLoache, B. Cervantes, J. E. Dueber, A highly characterized yeast toolkit for modular, multipart assembly. *ACS Synth. Biol.* **4**, 975–986 (2015).
47. C. Yan, H. Chen, L. Bai, Systematic study of nucleosome-displacing factors in budding yeast. *Mol. Cell* **71**, 294–305.e4 (2018).
48. B. Langmead, S. L. Salzberg, Fast gapped-read alignment with Bowtie 2. *Nat. Methods* **9**, 357–359 (2012).
49. E. A. Sekinger, Z. Moqtaderi, K. Struhl, Intrinsic histone-DNA interactions and low nucleosome density are important for preferential accessibility of promoter regions in yeast. *Mol. Cell* **18**, 735–748 (2005).